Paul Schoenhagen, MD
Sandra S. Halliburton, PhD
Arthur E. Stillman, MD, PhD
Stacie A. Kuzmiak, RT, CT(R)
Steven E. Nissen, MD
E. Murat Tuzcu, MD
Richard D. White, MD

Index terms:
Computed tomography (CT), angiography, 54.12111, 54.12112, 54.12115, 54.12116
Computed tomography (CT), multi–detector row, 54.12111, 54.12115, 54.12117, 54.12118, 54.12119
Coronary vessels, bypass graft, 54.4544
Coronary vessels, calcification, 54.812
Coronary vessels, CT, 54.12111, 54.12115, 54.12116, 54.12117, 54.12118, 54.12119
Coronary vessels, stenosis or obstruction, 54.4558, 54.76
Review

Published online
10.1148/radiol.2321021803
Radiology 2004; 232:7–17

Abbreviations:
CAD = coronary artery disease
ECG = electrocardiographic
LAD = left anterior descending

[1] From the Departments of Radiology (P.S., S.S.H., A.E.S., S.A.K., R.D.W.), Cardiovascular Medicine (P.S., S.E.N., E.M.T., R.D.W.), and Thoracic and Cardiovascular Surgery (R.D.W.), Cleveland Clinic Foundation, Desk Hb 6, 9500 Euclid Ave, Cleveland, OH 44195. Received December 30, 2002; revision requested April 11, 2003; revision received April 17; accepted May 1. Supported by an unrestricted training grant from Berlex Laboratories, Pine Brook, NJ. P.S. supported by a postdoctoral fellowship award from the Ohio Valley Regional Affiliate of the American Heart Association. **Address correspondence to** R.D.W. (e-mail: *whiter1@ccf.org*) or P.S. (e-mail: *schoenp1@ccf.org*).

Noninvasive Imaging of Coronary Arteries: Current and Future Role of Multi–Detector Row CT[1]

While invasive imaging techniques, especially selective conventional coronary angiography, will remain vital to planning and guiding catheter-based and surgical treatment of significantly stenotic coronary lesions, the comprehensive and serial assessment of asymptomatic or minimally symptomatic stages of coronary artery disease (CAD) for preventive purposes will eventually need to rely on noninvasive imaging techniques. Cardiovascular imaging with tomographic modalities, including computed tomography (CT) and magnetic resonance imaging, has great potential for providing valuable information. This review article will describe the current and future role of cardiac CT, and in particular that of multi–detector row CT, for imaging of atherosclerotic and other pathologic changes of the coronary arteries. It will describe how tomographic coronary imaging may eventually supplement traditional angiographic techniques in understanding the patterns of atherosclerotic CAD development.

EDITOR'S NOTE: In view of the importance of this topic, we are publishing in this issue of Radiology *two Special Reviews on CT evaluation of the coronary arteries. Each article presents important perspectives for our readers. Please see also the article by Schoepf et al.*

—Anthony V. Proto, MD, Editor

Since its introduction in the 1960s, selective coronary angiography has largely defined our understanding of normal and pathologic coronary anatomy (1–3). The precise angiographic definition of reduced luminal dimensions remains the basis for catheter-based or surgical revascularization of the myocardium in the distribution of significantly diseased coronary arteries. However, it is now appreciated that the accumulation of atherosclerotic plaque in the coronary arterial wall begins much earlier than the development of luminal stenosis. In fact, most acute coronary syndromes are initiated by sudden disruption of atherosclerotic plaques that are not causing significant stenosis (4). Therefore, the assessment of these early stages of coronary artery disease (CAD) has emerged as an important goal in preventing both CAD progression and complications of atherosclerotic CAD (eg, myocardial infarction) (5). Because early atherosclerotic plaque accumulation is typically associated with compensatory vessel expansion (positive arterial remodeling), the description of these important early changes of CAD on the basis of alterations in coronary luminal dimensions alone is not sufficient (6).

Intravascular ultrasonography (US), typically performed during selective coronary angiography, has allowed visualization of the coronary arterial wall and direct assessment of atherosclerotic plaque formation. While invasive techniques will remain vital to the diagnosis and treatment of significantly stenotic coronary lesions, the comprehensive and serial assessment of asymptomatic or minimally symptomatic stages of CAD for preventive purposes will eventually need to rely on noninvasive imaging techniques (7). Cardiovascular imaging with tomographic modalities, including computed tomography (CT) and magnetic resonance (MR) imaging, has great potential for providing this information (8).

ESSENTIALS

- *Unenhanced CT is very sensitive in detection and quantification of coronary arterial calcification, while contrast-enhanced CT can aid in differentiation of calcified and noncalcified plaque and in assessment of luminal stenosis.*
- *Multi–detector row CT angiography has a complementary diagnostic role in the assessment of patients with symptomatic CAD.*
- *The noninvasive characterization and quantification of atherosclerotic plaque burden may have important implications for the prevention of CAD progression and its complications.*

OVERVIEW OF CARDIAC CT

In contrast to imaging of all other organs, imaging of the heart must be performed during a fast and complex cyclical motion with substantial beat-to-beat variation. Therefore, image acquisition requires a high temporal resolution (time needed to acquire one image) and must be referenced to the cardiac cycle. The temporal resolution of CT (50–300 msec) is substantially lower than that of conventional angiography (<10 msec). To reduce cardiac motion artifacts, image acquisition should therefore be performed during a period of minimal cardiac movement, which is typically a brief interval in late diastole. In addition to high temporal resolution, high spatial resolution is essential for the visualization of cardiac anatomy, especially the anatomy of the coronary arteries. Image acquisition with this high temporal and spatial resolution should optimally cover the entire heart in a single breath hold to eliminate respiratory motion artifact.

Currently, two competing CT technologies, electron-beam CT and mechanical multi–detector row CT, are used for noninvasive cardiac imaging. Electron-beam CT has been developed by a single manufacturer (Imatron, South San Francisco, Calif) almost specifically for cardiac imaging because of its high temporal resolution (9). Electron-beam CT scanners use a rapidly rotating electron beam, which is reflected onto a stationary tungsten target. This technology can achieve temporal resolutions of 50–100 msec. Cardiac imaging with electron-beam CT is typically performed in sequential mode, where single transverse sections are sequentially acquired while the patient table is incrementally advanced. Data acquisition is prospectively referenced to the cardiac cycle by using the electrocardiographic (ECG) signal to trigger image acquisition. Sequential images are usually obtained with a 3-mm section thickness during one breath hold; thinner sections (1.5 mm) can also be obtained but increase scan time to 80–100 seconds, resulting in an acquisition over at least two breath-hold periods and increased respiratory motion artifact.

While the majority of coronary CT imaging has to date been performed by using electron-beam CT, recent technical advances in mechanical multi–detector row CT systems have enabled the noninvasive assessment of coronary arteries with this latter technology. Mechanical CT, which was originally developed for body imaging, is limited by the requirement of mechanical rotation of an x-ray tube around the patient. With initial single-section technology, the acquisition time for each image was 1–2 seconds, which introduced substantial cardiac motion artifact and prevented coverage of the entire heart in a single breath hold. However, the introduction of multi–detector row CT technology enabled the simultaneous acquisition of multiple sections per rotation. Coupled with decreased rotation times of the x-ray tube, current multi–detector row CT scanners allow high-temporal- and high-spatial-resolution imaging of large two-dimensional sequential or true three-dimensional volumetric series in a single breath hold (10).

Mechanical multi–detector row CT scanners have been developed by several manufacturers (General Electric, Phillips, Siemens, and Toshiba). State-of-the-art multi–detector row CT technology permits the acquisition of four to 16 anatomic sections per rotation (11–13). Cardiac multi–detector row CT imaging is performed either in a sequential mode, where the patient table is moved incrementally between successive rotations of the x-ray tube, or more often in a spiral mode, where the patient table is moved continuously during continuous rotation of the x-ray tube. Data acquisition is referenced to the ECG signal in a prospectively triggered or a retrospectively gated mode for sequential or spiral imaging methods, respectively. With gantry rotation speeds of 500 msec per rotation and the use of partial scan reconstruction algorithms, image acquisition times of 250–300 msec can be obtained with four–detector row systems. The minimum section thickness of cardiac four–detector row CT systems varies from 1.25 to 3.0 mm, depending on the clinical indication and the chosen method of image acquisition. Regardless of section thickness, data are obtained in a single breath hold. The recently introduced 16–detector row systems enable faster scanning (420 msec per rotation with 210-msec temporal resolution) and thinner image sections (0.75 mm) and are already showing improvements in cardiac imaging with mechanical multi–detector row CT (12,13). For patients with higher heart rates (>70 beats per minute), segmented reconstruction algorithms that utilize data from more than one cardiac cycle are frequently used with spiral imaging to reduce the effective temporal resolution to as low as 125 msec for four–detector row systems and 105 msec for 16–detector row systems (14,15). However, if possible, pharmacologic control of elevated heart rates is preferred (12,13).

While electron-beam CT has the advantage of better temporal resolution, multi–detector row CT offers a higher signal-to-noise ratio, shorter scan time, and higher spatial resolution. The lower signal-to-noise ratio with electron-beam CT is a result of limited x-ray intensity with use of this technology. Multi–detector row CT scanners can achieve higher tube currents, with subsequent improvement in image quality but also with increased radiation dose to the patient (16). To maintain the improved image quality while reducing radiation dose, current multi–detector row CT scanners may operate with fluctuating tube currents (dose modulation). With this approach, the maximal tube current is used only during a brief diastolic window, which corresponds to the period of minimal cardiac motion. As a general principle, multi–detector row CT tube current is chosen to achieve the level of image quality required to satisfy the clinical indication with an acceptable radiation exposure. The radiation exposure with multi–detector row CT, therefore, depends on the type of study performed.

CT imaging without intravascular contrast enhancement is used for the purpose of coronary artery calcium quantification. Calcium can be readily identified because of its high x-ray attenuation coefficient, or CT number measured in Hounsfield units. For calcium scoring, a threshold of 90 or 130 HU is applied to the entire image set (17,18). Tissues with an attenuation coefficient equal to or

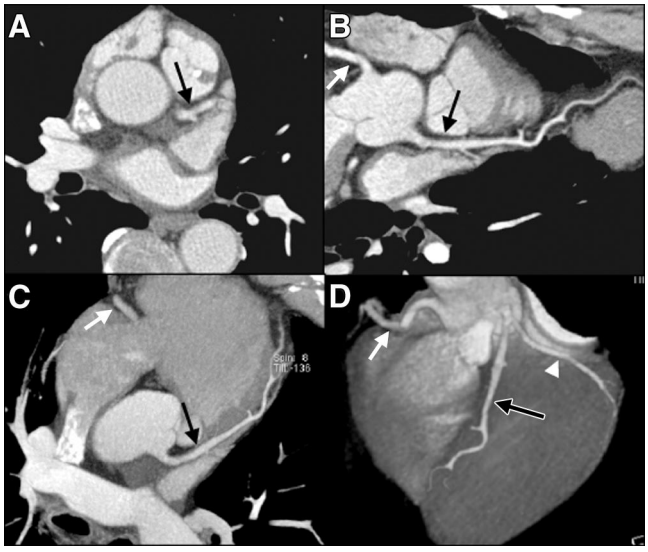

Figure 1. Normal coronary arteries at four–detector row CT. *A,* Transverse base image, *B,* transverse curved multiplanar reconstruction, *C,* oblique transverse thin maximum intensity projection, and *D,* left anterior oblique volume-rendered surface reconstruction demonstrate normal-appearing LAD coronary artery (black arrows). Proximal segments of right coronary artery (white arrows) and left circumflex coronary artery (arrowhead), which are also free of atherosclerotic changes, are seen.

Figure 2. Coronary artery with complex atherosclerotic plaque at four–detector row CT. *A,* Transverse base image, *B,* craniocaudal curved multiplanar reconstruction, *C,* oblique transverse thin maximum intensity projection, and *D,* left anterior oblique volume-rendered surface reconstruction demonstrate extensive atherosclerotic changes affecting LAD coronary artery, which contains a long complex plaque with calcified and noncalcified components (brackets) in its proximal segment. Proximal segments of right coronary artery (black arrow) and left circumflex coronary artery (white arrows), which also show irregularity and narrowing from atherosclerosis, are seen.

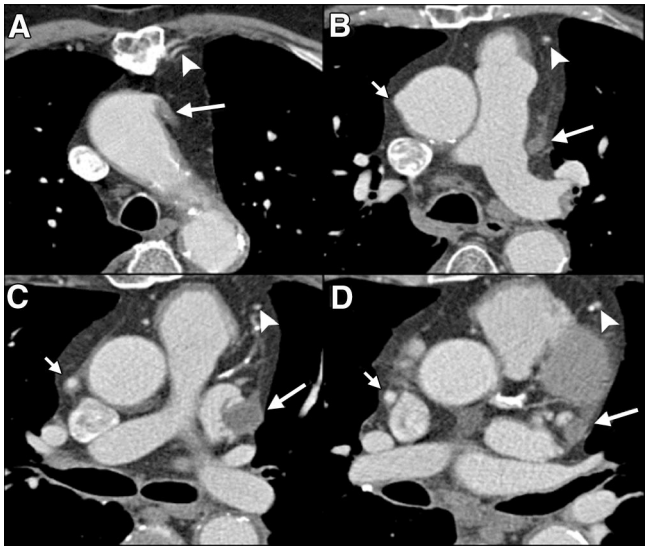

Figure 3. Coronary artery bypass graft status at four–detector row CT. *A–D,* Transverse cranial to caudal base images demonstrate occlusion of a dilated aortocoronary venous graft (large arrows) to the left circumflex coronary artery, while another aortocoronary venous graft (small arrows) communicating with the right coronary artery is patent. Left internal mammary artery graft (arrowheads) to the LAD coronary artery is also patent.

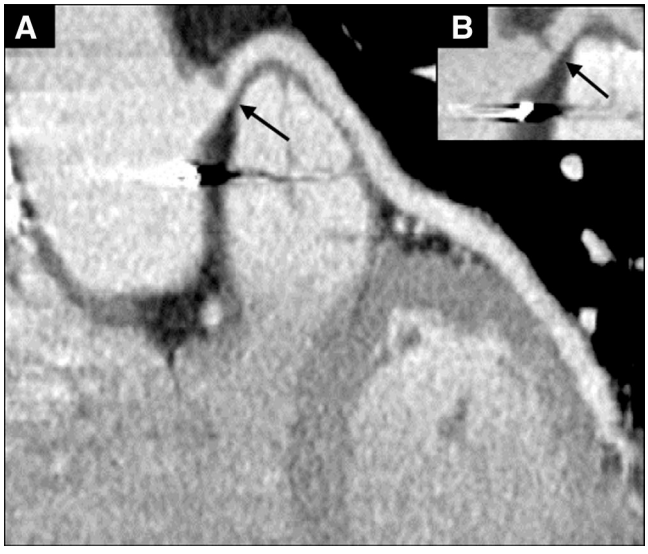

Figure 4. Progressing stenosis of coronary artery bypass graft at four–detector row CT. *A,* Craniocaudal curved multiplanar reconstruction and, *B,* corresponding 12-month follow-up image demonstrate focal asymmetric narrowing (arrows) of the proximal portion of aortocoronary venous graft to the middle left circumflex coronary artery. Initial ~70% narrowing progressed to ~90% narrowing and was accompanied by worsening angina.

greater than the selected threshold are identified as calcified lesions. Total calcium load in the entire coronary arterial tree can then be quantified from CT images by using one of several calcium scoring algorithms. Electron-beam CT is a well-established method for coronary calcium detection and is currently considered the standard. However, multi–de-

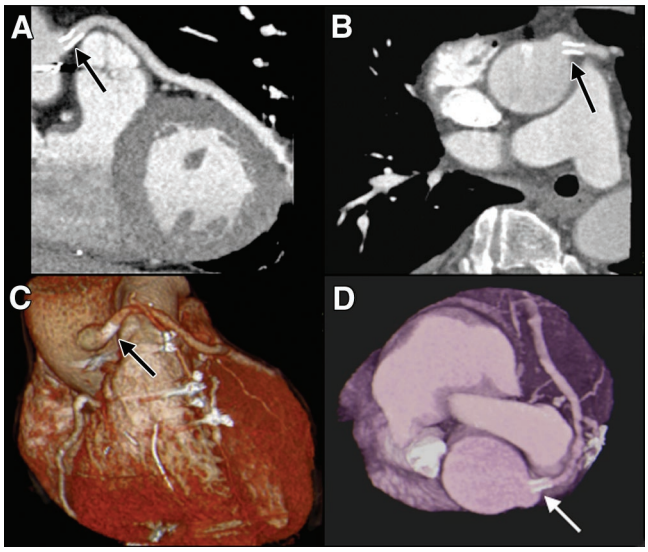

Figure 5. Coronary artery bypass graft stent patency at four–detector row CT. *A,* Craniocaudal curved multiplanar reconstruction, *B,* straight oblique transverse multiplanar reconstruction, *C,* uncropped anterior reconstruction, and *D,* cranially cropped volume-rendered surface reconstruction in the same patient as in Figure 4 demonstrate a widely patent stent (arrows) traversing the previously shown stenosis of the proximal portion of aortocoronary venous graft to the middle left circumflex coronary artery.

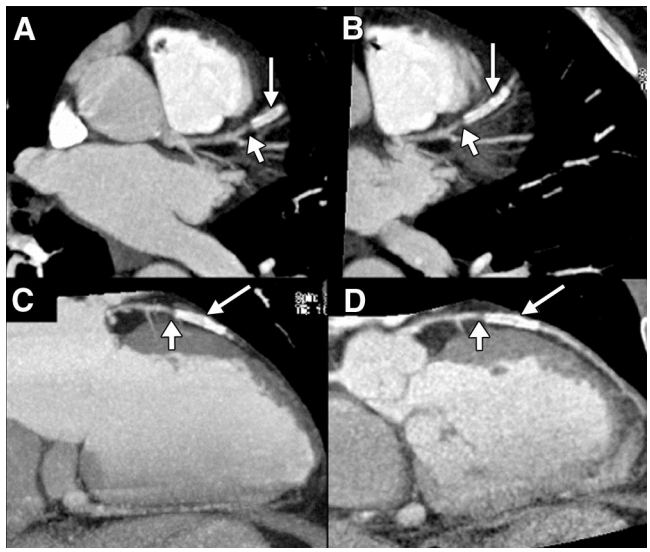

Figure 6. Coronary artery stent patency at four–detector row CT. Oblique transverse *(A, B)* and right anterior oblique *(C)* thin maximum intensity projections and craniocaudal curved multiplanar reconstruction *(D)* demonstrate short series of sequential stents (large arrows) within the middle LAD coronary artery. Stent patency is supported by prompt flow to distal segments of the artery. At the leading edge of the stent series, stenosis (small arrows) of the artery is noted.

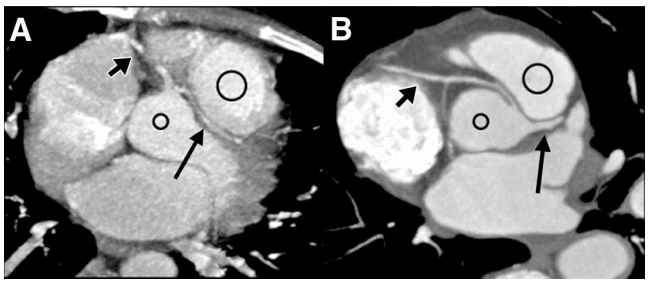

Figure 7. Anomalous coronary arteries at four–detector row CT. Thin oblique transverse maximum intensity projections in two patients with intermittent chest discomfort demonstrate anomalous origin and course of a major coronary artery between aortic root (small circles) and outflow tract of the right ventricle (large circles), resulting in compression and distortion of the artery. *A,* Anomalous LAD coronary artery (large arrow) has a common origin with the dominant right coronary artery (small arrow) from the right coronary sinus of Valsalva. *B,* Anomalous right coronary artery (small arrow) originates directly from the left coronary sinus of Valsalva, separately from the left coronary artery system (large arrow).

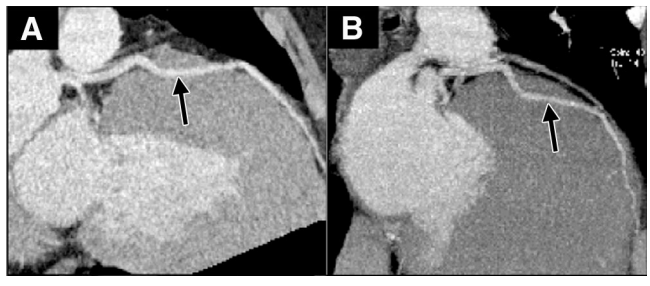

Figure 8. Coronary myocardial bridge at four–detector row CT. *A,* Craniocaudal curved multiplanar reconstruction and, *B,* thin right anterior oblique maximum intensity projection in a symptomatic patient demonstrate intramyocardial course (arrows) of middle portion of the otherwise normal-appearing LAD coronary artery. The overlying myocardium represents the bridge.

tector row CT has recently emerged as an alternative method for calcium detection and quantification (19).

To differentiate vessel lumen from vessel wall at CT, intravascular contrast-enhancement protocols are used. These CT protocols allow both angiographic evaluation of the coronary artery lumen and characterization of the coronary artery wall. Coronary CT angiography was initially described with use of electron-beam CT (20–24) but is increasingly performed with use of multi–detector row CT (12,13,25,26). Most experience with vessel wall and plaque characterization has been derived from studies with multi–detector row CT (27,28).

The analysis, interpretation, and documentation of coronary CT examinations are complex and not sufficiently standardized. Because of the tortuous course of coronary arteries, review of the acquired transverse image sections is often not sufficient. By using interactive three-dimensional reformation software, oblique planes can be displayed following the major cardiac axes and the course of individual coronary arteries. Coronary arteries are typically divided into smaller segments according to accepted angiographic classifications (29). These segments are then individually analyzed in longitudinal and cross-sectional planes (30). Diagnosis of luminal stenosis and vessel wall changes relies on these two-dimensional projections. Advanced image procession permits display of the entire three-dimensional data set by assigning different

Assessment of Luminal Stenosis Greater than 50%

Modality and Study	No. of Patients	Segments Excluded from Analysis (%)	Sensitivity (%)	Specificity (%)
Coronary electron-beam CT				
Reddy et al (21)	23	10	88	63
Budoff et al (22)	52	11	78	91
Schmermund et al (23)	28	28	82	88
Achenbach et al (24)	125	25	92	94
Four–detector row CT				
Nieman et al (25)	35	27	83	90
Achenbach et al (26)	64	32	85	76
16–detector row CT				
Nieman et al (12)	59	0*	95	86
Ropers et al (13)	77	12	92	93
MR angiography				
Kim et al (35)	109	16	93	42
van Geuns et al (36)	38	31	68	97
Regenfus et al (37)	50	23	86	91

* In contrast to other studies, sensitivity and specificity were calculated for all segments even if not evaluable with multi–detector row CT.

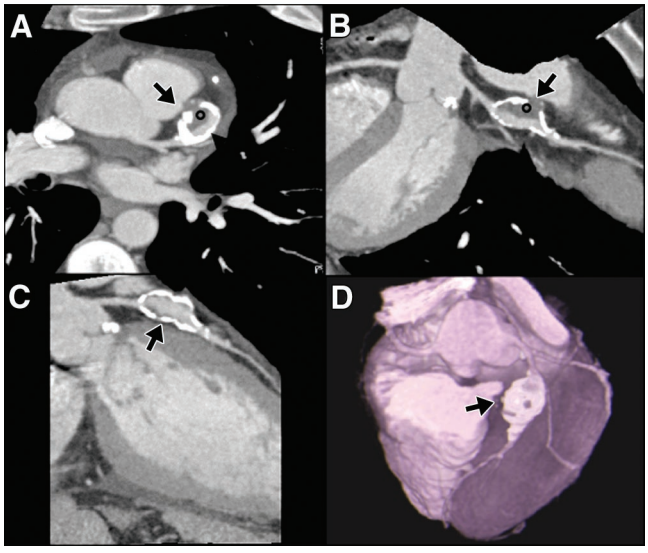

Figure 9. Coronary artery aneurysm (Kawasaki disease) at four–detector row CT. *A,* Oblique transverse thin maximum intensity projection, *B, C,* craniocaudal curved multiplanar reconstructions, and *D,* left anterior oblique volume-rendered surface reconstruction demonstrate calcified fusiform aneurysm (arrows) of the proximal middle LAD coronary artery containing thrombus (circles).

levels of transparency. These volume-rendered images facilitate the assessment of spatial orientation but provide only limited information about the arterial lumen and the vessel wall.

On the basis of our experience with multi–detector row CT, we will describe how cardiac CT might supplement traditional angiographic techniques in both understanding of the patterns of atherosclerotic CAD development and detection of other coronary arterial abnormalities of clinical importance.

DIAGNOSTIC CHALLENGES AND RELATED EXPERIENCE WITH CT OF CORONARY ARTERIES

Angiographic Display of Coronary Anatomy in Symptomatic Patients

Advanced CAD is characterized by multiple stenotic lesions of variable severity causing chronically reduced coronary blood flow and potentially gradual or sudden vessel occlusion. Consequently, advanced disease is clinically manifested by a wide variety of disease states, including stable angina pectoris, chronic heart failure, or acute coronary syndromes. In these clinical situations with a high pretest likelihood of significant stenotic atherosclerotic disease, the definitive identification and accurate quantification of luminal stenoses in the entire epicardial coronary tree are necessary. Selective conventional angiography provides this information with high spatial (0.1-mm) and temporal (4–7-msec) resolution and allows simultaneous catheter-based therapeutic interventions (angioplasty, stent placement). Therefore, selective angiography will remain vital for guiding interventional or surgical (bypass grafting) treatment of significantly stenotic coronary lesions. However, in other clinical situations, the comprehensive assessment of obstructive and nonobstructive CAD may eventually increasingly rely on noninvasive imaging techniques.

Coronary angiography with use of multi–detector row CT is typically performed in a spiral scan mode, which permits three-dimensional scanning of the entire heart in a single breath hold (31). Data are retrospectively referenced to the ECG signal to reconstruct images during the diastolic phase of the cardiac cycle (32). Adjacent overlapping transverse images are reconstructed with a minimum section thickness of as little as 0.75 mm and a maximum in-plane spatial resolution of approximately 0.4×0.4 mm. Patient radiation dose at multi–detector row CT angiography is similar to that at conventional coronary angiography (3.5–6.5 mSv) (16).

For the diagnostic evaluation of coronary arteries, the acquired transverse images may be reformatted into images following the major axes of the cardiac chambers or the course of individual coronary arteries (30). Various reformatting techniques (multiplanar reconstruction, maximum intensity projection, or volume rendering) are used, depending on the clinical indication.

With multi–detector row CT angiography, complete visualization of all segments of the epicardial coronary arteries is limited by cardiac motion, the small size of distal arterial segments, and the tortuous course of these vessels through the imaging plane. Because the left main coronary artery and proximal portions of the left anterior descending (LAD) artery experience the least motion and run approximately parallel to the acquired transverse plane, these segments are most reliably visualized with multi–detector row CT angiography (Figs 1, 2). On

the other hand, the consistent and reproducible visualization of the right coronary artery, the circumflex coronary artery, and the small side branches is difficult because of these vessels' complex motion during the cardiac cycle and oblique orientations to the imaging plane. Study findings have demonstrated the advantage of retrospectively reconstructing data in different phases of the cardiac cycle for optimal visualization of different coronary arteries (33,34).

In one study (26), 68% of all coronary arterial segments could be visualized at four–detector row CT angiography. In these analyzable segments, the sensitivity and specificity in the detection of significant luminal stenosis in comparison with those of conventional angiography were 91% and 84%, respectively, which were similar to those in previous reports (20–25). Authors of studies using state-of-the-art 16–detector row system report similar sensitivity and specificity but improved visualization, with about 10% of poorly assessable segments (12,13). The Table summarizes results from representative clinical studies in which electron-beam CT, multi–detector row CT, and MR angiography were used for the assessment of significant coronary luminal stenosis. It is important to emphasize that authors of most studies calculate sensitivity and specificity based on the results in analyzable segments rather than on those of all examined segments. A well-recognized limitation in the assessment of coronary stenosis with CT angiography is related to partial volume averaging of coronary arterial calcification. The attenuation coefficient of a given voxel containing even a small portion of calcium is typically dominated by the high attenuation coefficient of calcium. The resulting "blooming" effect of coronary arterial calcification causes difficulties in assessing adjacent plaque structures, potentially resulting in a false-positive detection of stenosis or overestimation of the degree of narrowing (25).

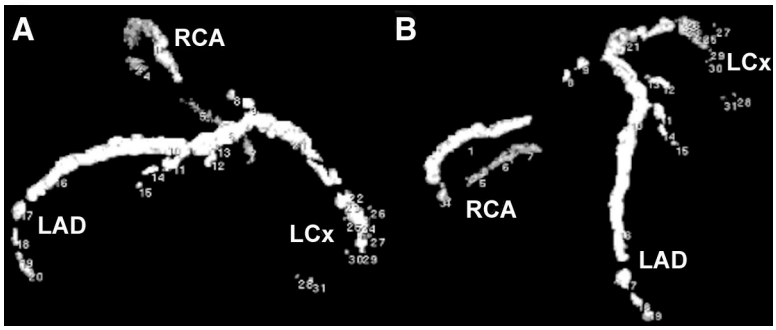

Figure 10. Coronary calcification scoring. *A,* Left lateral and, *B,* left anterior oblique projections of the distribution of plaques detected (numbered) during scoring of atherosclerotic coronary calcification with nonenhanced four–detector row CT. Because of the extent of coronary calcification, outlines of LAD, left circumflex *(LCx),* and dominant right *(RCA)* coronary arteries are formed.

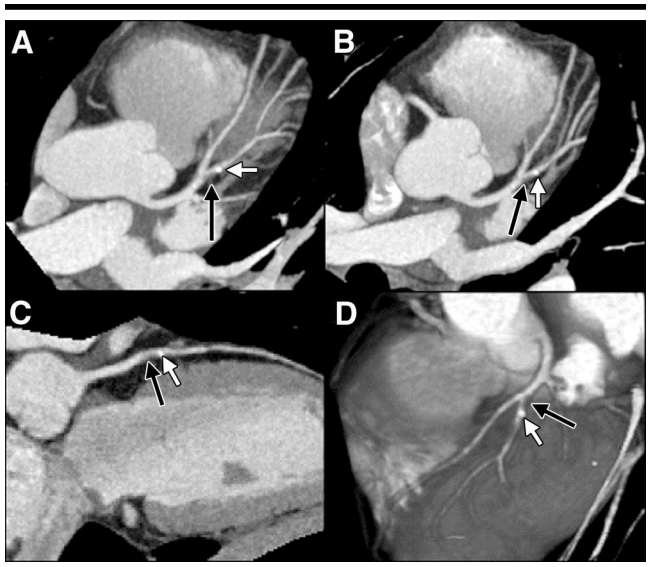

Figure 11. Soft, noncalcified, atherosclerotic plaque at four–detector row CT. *A, B,* Oblique transverse thin maximum intensity projections, *C,* craniocaudal curved multiplanar reconstruction, and *D,* left anterior oblique volume-rendered surface reconstruction demonstrate multiple noncalcified atherosclerotic plaques within the LAD coronary artery system, which result in focal arterial wall thickening with mild narrowing of the coronary lumen. Best example is noted in proximal portion of a major diagonal branch, where a prominent soft plaque (black arrows), followed by a small nodular collection of calcification (white arrows), is seen.

Serial follow-up examinations after catheter-based or surgical myocardial revascularization currently rely on selective coronary angiography and functional stress tests. CT angiography has been advocated for these clinical situations, but the existing data are preliminary. Several reports have described the assessment of bypass grafts with use of CT angiography (38,39). Patency or occlusion of grafts can be established by the presence or absence of contrast enhancement, respectively (Fig 3). Because of their relatively large size compared with that of internal mammary grafts, venous aortocoronary grafts can also be evaluated for the presence and severity of stenosis (Fig 4). While artifact from metallic surgical clips may obscure the adjacent portion of a coronary graft, a common situation for internal mammary grafts, interference tends to be less than that found on MR images. Similar to surgical clips, the high-attenuation metallic mesh of coronary stents precludes confident detection and grading of in-stent restenosis with CT due to partial volume averaging. However, differentiation between stent patency and occlusion (Fig 5) and evaluation of stenosis at the leading or trailing ends of a stent are possible (Fig 6). In addition, stent patency can be inferred on the basis of the presence or absence of coronary luminal enhancement distal to the stent (40).

An important advantage of multi–detector row CT angiography over conventional angiography is that additional information about cardiac and noncardiac anatomy is simultaneously provided. An important clinical differentiation is that between stenotic atherosclerotic CAD

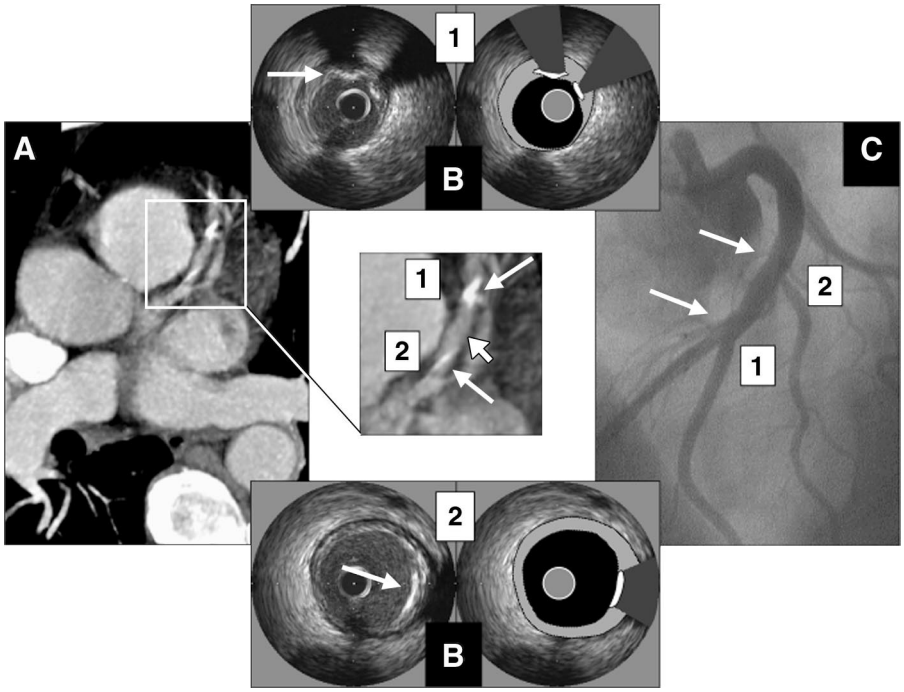

Figure 12. Correlative atherosclerotic plaque characterization. Comparison between, *A,* four–detector row CT, *B,* intravascular US, and *C,* left anterior oblique selective conventional angiography for atherosclerotic plaque formation in proximal middle LAD coronary artery. *A,* Oblique transverse thin maximum intensity projection shows coronary arterial wall calcification at two plaque sites (large arrows), most notably at site 1, with interposed positive remodeling (small arrow). Center image is an enlargement of boxed area in *A*. Reliable assessment of luminal dimension at sites of calcification is not possible because of the "blooming" artifact. In contrast, *C* confirms absence of significant stenosis but provides poor definition of arterial wall changes (arrows). *B,* Intravascular cross-sectional native (left) and illustrated (right) US images at sites 1 (top) and 2 (bottom) demonstrate calcified plaque without significant narrowing. Illustrations demonstrate the catheter (light gray) in the center of the lumen (black), which is surrounded by the vessel wall (dark gray). Calcified plaque in the vessel wall causes a characteristic signal void termed *calcium shadow*.

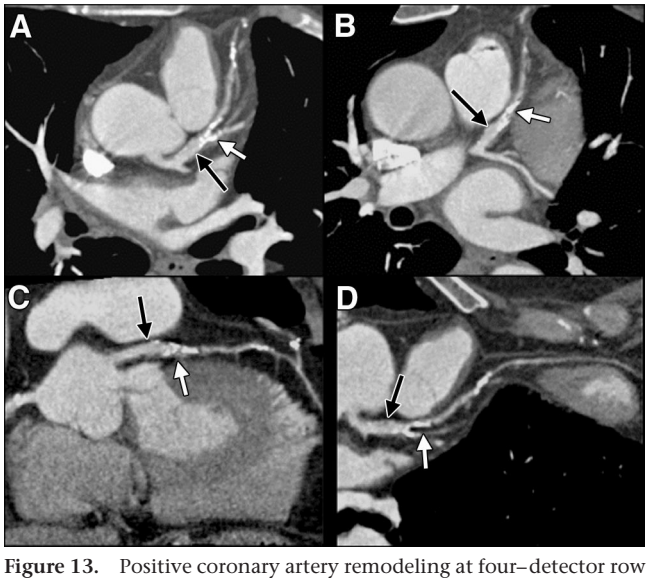

Figure 13. Positive coronary artery remodeling at four–detector row CT. *A, B,* Oblique transverse thin maximum intensity projections and, *C,* craniocaudal and, *D,* transverse curved multiplanar reconstructions demonstrate ectasia (black arrows) of the proximal LAD coronary artery, with irregularity of arterial wall due to early atherosclerotic plaque formation. The segment is followed by a densely calcified segment (white arrows) with luminal narrowing.

and anomalous origin and/or course of a coronary artery (41). Tracking of a congenitally abnormal coronary artery through several image planes by using the original image set or image reformations defines the relation of the anomalous coronary artery to other cardiovascular structures. This information is of great clinical importance because, for example, the demonstration of an anomalous artery tracking between the aorta and the pulmonary artery (Fig 7) may define an indication of surgical correction. Additional nonatherosclerotic coronary abnormalities detectable at multi–detector row CT angiography include the intramyocardial course of a coronary artery due to a myocardial bridge (Fig 8) and aneurysmally dilated coronary arteries (Fig 9) with or without thrombus.

In summary, because of higher spatial and temporal resolution and complete depiction of the entire epicardial tree, selective angiography will remain vital for the diagnosis and treatment of CAD in symptomatic patients. However, multi–detector row CT angiography potentially has a complementary diagnostic role in these clinical situations. It is important to understand that the lower spatial resolution of CT angiography is more problematic in the assessment of highly stenotic lesions; a subtotal coronary occlusion with a lumen size below the resolution of CT cannot be differentiated from a total occlusion. On the other hand, CT angiography has the advantage of vessel wall and plaque depiction in addition to its ability to enable assessment of luminal dimensions. The assessment of size and composition (eg, calcification) of coronary arterial lesions and the associated changes in vessel architecture (eg, arterial remodeling) may have important clinical implications.

Plaque Burden Assessment and Plaque Characterization in Asymptomatic or Minimally Symptomatic Patients

The number of significant stenoses in the coronary arterial tree as assessed with selective conventional angiography has prognostic value. However, serial angiographic observations of existing severe stenoses do not allow the assessment of the effect of risk-factor modification. Generally, changes in atherosclerotic plaque size are not well reflected in luminal dimensions, because plaque progression and regression are associated with arterial expansion (positive remodeling) and shrinkage (negative remodeling)

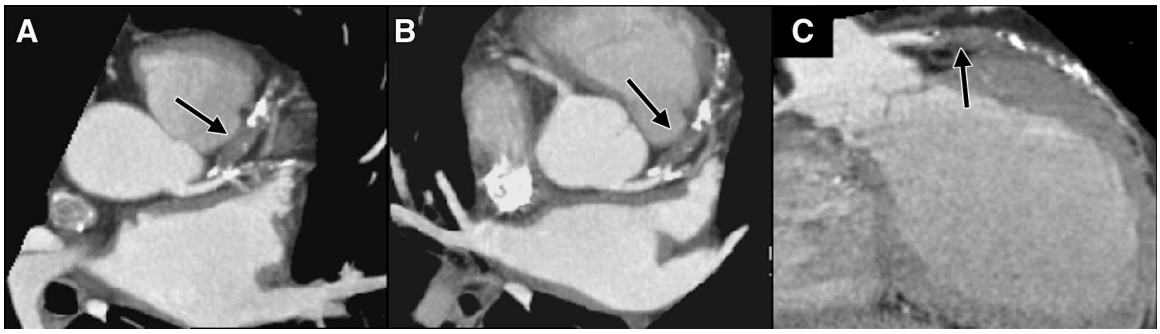

Figure 14. Thrombotic coronary occlusion at the site of positive remodeling at four–detector row CT. *A, B,* Oblique transverse thin maximum intensity projections and, *C,* craniocaudal curved multiplanar reconstruction demonstrate complete filling with thrombus of the ectatic lumen (arrows) of mildly calcified proximal LAD coronary artery.

(42,43). This limitation of angiographic lesion assessment has become evident from prevention trials with lipid-lowering medications that showed a statistically significant reduction in clinical events but only minimal change in the severity of existing angiographic stenoses. In addition, findings of several studies have shown that most acute coronary syndromes are initiated by sudden changes of mildly stenotic lesions, commonly found in positively remodeled arterial regions, rather than from progression of lesions already causing significant luminal narrowing (44–46). Therefore, it has been postulated that the identification of mildly stenotic but vulnerable atherosclerotic lesions and the overall plaque burden could provide better markers of coronary risk than do measures of luminal stenosis (47). This hypothesis is currently being examined in intravascular US studies (48), but eventually noninvasive imaging techniques would be needed for clinical applications in CAD prevention. Multi–detector row CT has a potential to address several important parameters about early atherosclerotic changes in the coronary arteries.

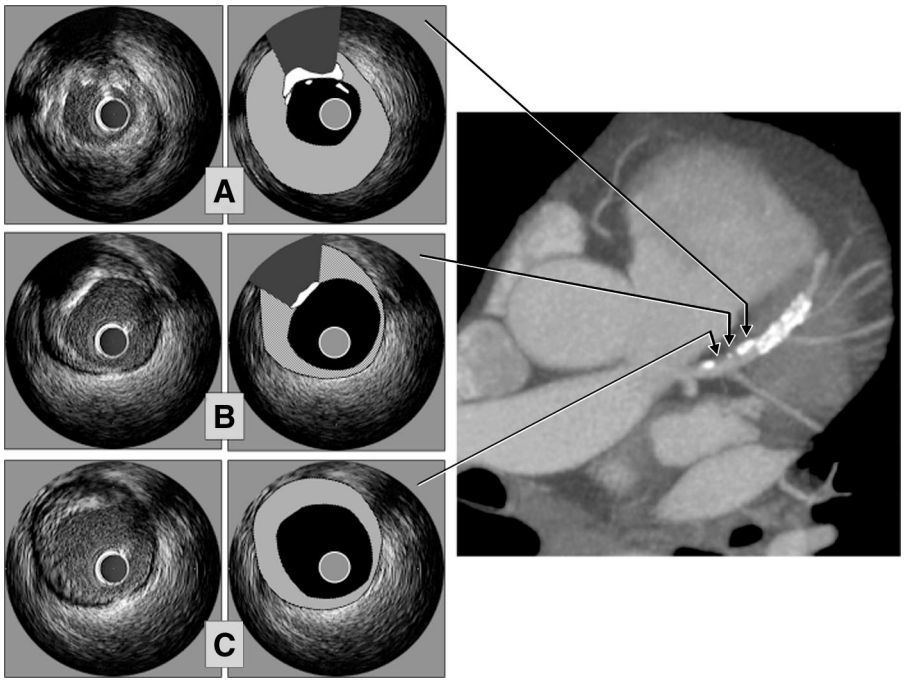

Figure 15. Comparison of calcified and noncalcified coronary atherosclerotic plaque. Individual cross-sectional intravascular US images (*A–C*) and a corresponding oblique transverse thin maximum intensity projection from 16–detector row CT angiography data set (right) demonstrate atherosclerotic plaque just proximal to a segment with stent in the proximal LAD. *A, B,* Calcified and, *C,* noncalcified components of the plaque are depicted; native (left) and illustrated (right) images at different sites in the vessel segment are shown. Illustrations demonstrate catheter (light gray) in the center of lumen (black), which is surrounded by vessel wall.

Assessment of plaque burden, including calcium scoring.—The identification of coronary arterial calcification is a reliable sign of chronic atherosclerotic changes of the coronary arterial tree (4). CT examinations performed without contrast material are very sensitive in detection and quantification of coronary arterial calcification and can enable noninvasive survey of the entire coronary tree (Fig 10).

Coronary calcium detection is routinely performed with electron-beam CT (9). Corresponding techniques with multi–detector row CT have typically used a prospectively ECG-triggered sequential scan mode (19), with acquisition of adjacent transverse image sections in diastole. Images covering the entire heart are obtained in a single breath hold, usually with a temporal resolution equal to 250 msec and a section thickness equal to 2.5 mm. By using multi–detector row CT with the sequential scan mode, patient radiation doses are equivalent to those of calcium scoring examinations with electron-bean CT (<1 mSv). X-ray exposure is higher for retrospectively ECG-gated spiral examinations, which acquire 30 data sets and allow reconstruction from overlapping images. The added value of acquiring spiral data for calcium scoring has not been demonstrated sufficiently, but these examinations may reduce the probability of misregistration of calcified lesions.

The traditional method of quantifying coronary artery calcium is the Agatston scoring system, which assigns a calcium score based on the maximum CT number

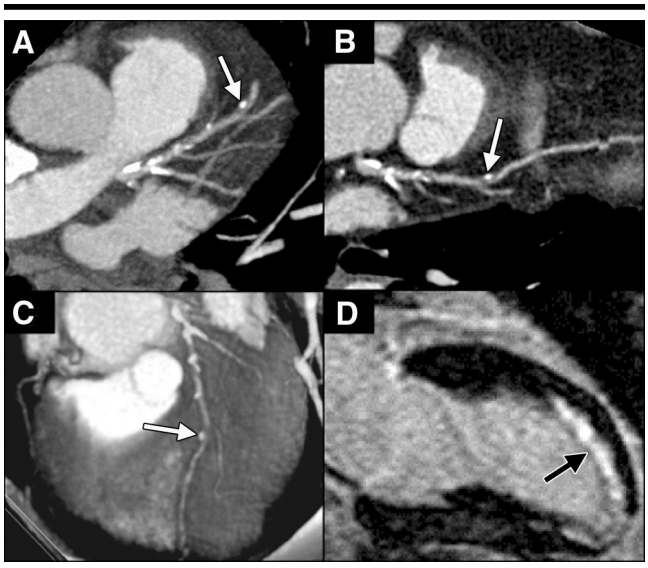

Figure 16. Correlation between patterns of coronary atherosclerosis and resulting myocardial necrosis. *A,* Oblique transverse thin maximum intensity projection, *B,* transverse curved multiplanar reconstruction, and *C,* left anterior oblique volume-rendered surface reconstruction at four–detector row CT in a patient with non–ST segment-elevation myocardial infarction demonstrate a potentially unstable combination of focal soft atherosclerotic plaque with a calcified nodule (arrows) within the middle LAD coronary artery. *D,* Two-chamber vertical long-axis delayed-enhancement 1.5-T MR image shows corresponding hyperintense region in the middle to apical left ventricular myocardium, which indicates subendocardial myocardial necrosis (arrow), despite distal patency of LAD coronary artery following thrombolytic therapy.

and the area of calcium deposits (17). Alternative methods of calcium scoring introduced more recently include volume scoring, which provides an estimate of the volume of calcium in cubic millimeters (49), and mass scoring, which represents the absolute mass of the calcium in milligrams (50).

Most information to date on the prognostic value of quantifying coronary arterial calcium has been derived from Agatston scores obtained by using electron-beam CT technology. Coronary calcium scores at electron-beam CT have been shown to correlate with the total atherosclerotic plaque burden (calcified and noncalcified plaque), although the absolute burden is substantially underestimated (51,52). The predictive value of calcium scores at electron-beam CT for significant coronary stenosis or future coronary events has been shown (53). Dynamic changes in the calcium volume score during pharmacologic therapy have been examined in serial electron-beam CT studies (54,55). Coronary plaque burden measured with CT coronary calcium scoring could potentially be used to assess the efficacy of preventive measures. Current prospective studies, in particular the Multi-Ethnic Study of Atherosclerosis of the National Heart, Lung, and Blood Institute, will assess the relationship between future clinical outcomes, traditional cardiovascular risk factors, and newer indicators of subclinical disease, including quantified coronary arterial calcium with electron-beam and multi–detector row CT, during a long-term follow-up (56). According to American Heart Association/American College of Cardiology consensus statement, the incremental value of calcium scores over traditional multivariate risk-assessment models has not yet been established (57). Consequently, these guidelines do not recommend routine CT screening of coronary arterial calcium in asymptomatic individuals, but conclude that screening is justified in selected patient groups with intermediate risk.

Assessment of plaque characteristics.—Calcium scoring helps identify the calcified portion of the overall atherosclerotic plaque burden; however, noncalcified atherosclerotic plaque (which in fact could have microcalcifications below the threshold of detection with calcium scoring techniques) may be more unstable and prone to rupture, causing acute coronary syndromes (58). The morphologic characteristics of unstable, or vulnerable, plaques are not completely understood. Differences between stable and unstable coronary plaques have been examined with coronary intravascular US, and hypoechoic plaque has been associated with the clinical presentation of unstable angina (59,60). Studies also demonstrate an association between acute coronary syndromes and positive remodeling (46,61). Authors of a prospective serial intravascular US study found that mildly stenotic coronary lesions exhibiting positive remodeling and a hypoechoic area at baseline have more frequently caused acute coronary syndromes during follow-up (61).

A noninvasive technique for the characterization and quantification of both calcified and noncalcified atherosclerotic plaque components would facilitate serial observations in clinical studies. Evidence of the ability of multi–detector row CT angiography techniques to help identify and characterize noncalcified plaques is emerging (27,28) (Figs 11, 12). Multi–detector row CT angiography has been compared with intravascular US for the differentiation between atherosclerotic coronary plaque components demonstrating sufficiently different attenuation levels (27). On the basis of comparison with common intravascular US plaque classification, soft plaques were characterized by a mean CT attenuation of 14 HU ± 26 (range, −42 to 47 HU); intermediate plaques, 91 HU ± 21 (range, 61–112 HU); and calcified plaques, 419 HU ± 194 (range, 126–736 HU).

Coronary segments with positive arterial remodeling (Fig 13) that harbor substantial amounts of noncalcified plaque without significant luminal stenosis can be detected with multi–detector row CT angiography. Positive remodeling can also be observed in combination with thrombotic occlusion (Fig 14), which supports the concept that remodeling and accumulation of noncalcified plaque early in the atherosclerotic process predispose to acute coronary events. To define the role of multi–detector row CT angiography for the identification of atherosclerotic plaque and characterization of plaque morphology and remodeling, future studies will need to compare multi–detector row CT, especially the emerging 16–detector row systems, with established invasive modalities that include intravascular US and emerging technologies such as optical coherence tomography (62) (Fig 15).

CONCLUSION

Imaging of coronary arteries with selective conventional angiography is focused on the severity of luminal stenosis. The assessment of advanced stages of CAD with selective angiography remains the basis for planning and guiding catheter-based and surgical myocardial revascularization treatment. In contrast, prevention of coronary events requires identification of early stages of disease and the associated abnormalities in coronary architecture before the development of luminal stenosis.

Invasive catheter-based diagnostic techniques, in particular intravascular US, allow visualization of a wide range of coronary lesions independent of their luminal dimensions. However, noninvasive coronary imaging techniques will eventually be necessary for the routine examination of asymptomatic or minimally symptomatic patients with moderate risk.

Noninvasive coronary imaging with CT technology, especially multi–detector row CT, can already be applied to both the assessment of significant luminal stenosis and the identification of nonstenotic atherosclerotic plaques. Multi–detector row CT angiography could become complementary to conventional angiography in the assessment of selected patients with stenotic atherosclerotic or nonatherosclerotic coronary disease. The noninvasive characterization and quantification of atherosclerotic plaque burden may have important implications for the prevention of CAD progression and/or its complications.

More important, CT techniques provide an overall assessment of cardiac anatomy beyond coronary imaging, paralleling morphologic capabilities of cardiac MR imaging (7,8,35–37,63). In centers where both angiographic and tomographic imaging modalities are available, the integration of tomographic image information will facilitate comprehensive noninvasive imaging of patients with early and those with late stages of CAD (Fig 16). The clinical impact of noninvasive tomographic imaging technologies, such as multi–detector row CT, on imaging of coronary arteriosclerosis will need further elucidation, but the prospects are exciting.

Acknowledgments: The authors thank the past and present members of the Siemens MDCT group for their technical support of this work. In particular, we express our appreciation to K. Hambuechen, R. Hausmann, MD, K. Klingenbeck-Regn, MD, S. Schaller, MD, J. Regn, MD, B. Ohnesorge, MD, T. Flohr, MD, and M. Petersilka, MD. Technical descriptions, imaging protocols, and example images included in this work are based on our experience to date with a four-section CT scanner (Somatom Volume Zoom; Siemens Medical Systems, Forchheim, Germany); we are currently utilizing both the four-section system and a new 16-section system (Sensation-16; Siemens Medical Systems). Comparable protocols with scanners from other manufacturers may vary slightly.

References

1. Sones FM Jr, Shirey EK. Cine coronary arteriography. Mod Concepts Cardiovasc Dis 1962; 31:735–738.
2. Ricketts HJ, Abrams HL. Percutaneous selective coronary cine arteriography. JAMA 1962; 181:620–623.
3. Judkins MP. Selective coronary arteriography: a percutaneous transfemoral technique. Radiology 1967; 89:815–817.
4. Ross R. The pathogenesis of atherosclerosis. Nature 1993; 362:801–809.
5. Libby P. Current concepts of the pathogenesis of the acute coronary syndromes. Circulation 2001; 104:365–372.
6. Topol EJ, Nissen SE. Our preoccupation with coronary luminology. Circulation 1995; 92:2333–2342.
7. Fayad ZA, Fuster V. Clinical imaging of the high-risk or vulnerable atherosclerotic plaque. Circ Res 2001; 89:305–316.
8. Fayad ZA, Fuster V, Nikolaou K, Becker C. Computed tomography and magnetic resonance imaging for noninvasive coronary angiography and plaque imaging: current and potential future concepts. Circulation 2002; 106:2026–2034.
9. Budoff MJ, Raggi P. Coronary artery disease progression assessed by electron-beam computed tomography. Am J Cardiol 2001; 88:46E–50E.
10. Fuchs T, Kachelriess M, Kalender WA. Technical advances in multi-slice spiral CT. Eur J Radiol 2000; 36:69–73.
11. Klingenbeck-Regn K, Schaller S, Flohr T, Ohnesorge B, Kopp AF, Baum U. Subsecond multi-slice computed tomography. Eur J Radiol 1999; 31:110–124.
12. Nieman K, Cademartiri F, Lemos PA, Raaijmakers R, Pattynama PMT, de Feyter PJ. Reliable noninvasive coronary angiography with fast submillimeter multislice spiral computed tomography. Circulation 2002; 106:2051–2054.
13. Ropers D, Baum U, Pohle K, et al. Detection of coronary artery stenoses with thin-slice multi-detector row spiral computed tomography and multiplanar reconstruction. Circulation 2003; 107:664–666.
14. Hu H, He HD, Foley WD, Fox SH. Four multidetector-row helical CT image quality and volume coverage speed. Radiology 2000; 215:55–62.
15. Halliburton SS, Stillman AE, Flohr T, et al. Do segmented reconstruction algorithms for cardiac multi-slice computed tomography improve image quality? Herz 2003; 28:20–31.
16. Cohnen M, Poll L, Puettmann C, Ewen K, Moedder U. Radiation exposure in multislice CT of the heart. Rofo Fortschr Geb Rontgenstr Neuen Bildgeb Verfahr 2001; 173:295–299.
17. Agatston AS, Janowitz WR, Hildner FJ, Zusmer NR, Viamonte M, Detrano R. Quantification of coronary artery calcium using ultrafast computed tomography. J Am Coll Cardiol 1990; 15:827–832.
18. Shemesh J, Apter S, Rozenman J, et al. Calcification of coronary arteries. Radiology 1995; 197:779–783.
19. Becker CR, Kleffel T, Crispin A, et al. Coronary artery calcium measurement: agreement of multirow detector and electron beam CT. AJR Am J Roentgenol 2001; 176:1295–1298.
20. Rensing BJ, Bongaerts A, van Geuns RJ, van Ooijen P, Oudkerk M, de Feyter PJ. Intravenous coronary angiography by electron beam computed tomography. Circulation 1998; 98:2509–2512.
21. Reddy GP, Chernoff DM, Adams JR, Higgins CB. Coronary artery stenoses: assessment with contrast-enhanced electron-beam CT and axial reconstructions. Radiology 1998; 208:167–172.
22. Budoff MJ, Oudiz RJ, Zalace CP, et al. Intravenous three-dimensional coronary angiography using contrast enhanced electron beam computed tomography. Am J Cardiol 1999; 83:840–845.
23. Schmermund A, Rensing BJ, Sheddy PF, Bell MR, Rumberger JA. Intravenous electron-beam computed tomographic coronary angiography for segmental analysis of coronary artery stenoses. J Am Coll Cardiol 1998; 31:1547–1554.
24. Achenbach S, Moshage W, Ropers D, Nossen J, Daniel WG. Value of electron-beam computed tomography for the noninvasive detection of high-grade coronary-artery stenoses and occlusions. N Engl J Med 1998; 339:1964–1971.
25. Nieman K, Oudkerk M, Rensing BJ, et al. Coronary angiography with multi-slice computed tomography. Lancet 2001; 357: 599–603.
26. Achenbach S, Giesler T, Ropers D, et al. Detection of coronary artery stenoses by contrast-enhanced, retrospectively electrocardiographically-gated, multislice spiral computed tomography. Circulation 2001; 103:2535–2538.
27. Schroeder S, Kopp AF, Baumbach A, et al. Noninvasive detection and evaluation of atherosclerotic coronary plaques with multislice computed tomography. J Am Coll Cardiol 2001; 37:1430–1435.
28. Becker CR, Knez A, Ohnesorge B, Schoepf UJ, Reiser MF. Imaging of noncalcified coronary plaques using helical CT with retrospective ECG gating. AJR Am J Roentgenol 2000; 175:423–424.
29. National Heart, Lung, and Blood Institute Coronary Artery Surgery Study. A multicenter comparison of the effects of randomized medical and surgical treatment of mildly symptomatic patients with coronary artery disease, and a registry of consecutive patients undergoing coronary angiography. Circulation 1981; 63(pt 2): I1–I81.
30. Gerber TC, Kuzo RS, Lane GE, et al. Image quality in a standardized algorithm for minimally invasive coronary angiography with multislice spiral computed tomography. J Comput Assist Tomogr 2003; 27:62–69.
31. Becker CR, Ohnesorge BM, Schroepf UJ, Reiser MF. Current development of cardiac imaging with multidetector-row CT. Eur J Radiol 2000; 36:97–103.
32. Ohnesorge B, Flohr T, Becker C, et al. Cardiac imaging by means of electrocar-

diographically gated multisection spiral CT. Radiology 2000; 217:564–571.
33. Hong C, Becker CR, Huber A, et al. ECG-gated reconstructed multi-detector row CT coronary angiography: effect of varying trigger delay on image quality. Radiology 2001; 220:712–717.
34. Kopp AF, Schroeder S, Kuettner A, et al. Coronary arteries: retrospectively ECG-gated multi-detector row CT angiography with selective optimization of the image reconstruction window. Radiology 2001; 221:683–688.
35. Kim WY, Danias PG, Stuber M, et al. Coronary magnetic resonance angiography for the detection of coronary stenoses. N Engl J Med 2001; 345:1863–1869.
36. van Geuns RJ, Wielopolski PA, de Bruin HG, et al. MR coronary angiography with breath-hold targeted volumes: preliminary clinical results. Radiology 2000; 217: 270–277.
37. Regenfus M, Ropers D, Achenbach S, et al. Noninvasive detection of coronary artery stenosis using contrast-enhanced three-dimensional breath-hold magnetic resonance coronary angiography. J Am Coll Cardiol 2000; 36:44–50.
38. Engelmann MG, von Smekal A, Knez A, et al. Accuracy of spiral computed tomography for identifying arterial and venous coronary graft patency. Am J Cardiol 1997; 80:569–574.
39. Dai R, Zhang S, Lu B, et al. Electron-beam CT angiography with three-dimensional reconstruction in the evaluation of coronary artery bypass grafts. Acad Radiol 1998; 5:863–867.
40. Lu B, Dai R, Bai H, et al. Detection and analysis of intracoronary artery stent after PTCA using contrast-enhanced three-dimensional electron beam tomography. J Invasive Cardiol 2000; 12:1–6.
41. Ropers D, Moshage W, Daniel WG, Jessl J, Gottwik M, Achenbach S. Visualization of coronary artery anomalies and their anatomic course by contrast-enhanced electron beam tomography and three-dimensional reconstruction. Am J Cardiol 2001; 87:193–197.
42. Glagov S, Weisenberg E, Zarins CK, Stankunavicius R, Kolettis GJ. Compensatory enlargement of human atherosclerotic coronary arteries. N Engl J Med 1987; 316:1371–1375.
43. Schoenhagen P, Ziada KM, Vince DG, Nissen SE, Tuzcu EM. Arterial remodeling and coronary artery disease: the concept of "dilated" versus "obstructive" coronary atherosclerosis. J Am Coll Cardiol 2001; 38:297–306.
44. Falk E, Shah PK, Fuster V. Coronary plaque disruption. Circulation 1995; 92: 657–671.
45. Little WC, Constantinescu M, Applegate RJ, et al. Can coronary angiography predict the site of a subsequent myocardial infarction in patients with mild-to-moderate coronary artery disease? Circulation 1988; 78:1157–1166.
46. Schoenhagen P, Ziada K, Kapadia SR, et al. Extent and direction of arterial remodeling in stable versus unstable coronary syndromes. Circulation 2000; 101:598–603.
47. Takagi T, Yoshida K, Akasaka T, Hozumi T, Morioka S, Yooshikawa J. Intravascular ultrasound analysis of reduction in progression of coronary narrowing by treatment with pravastatin. Am J Cardiol 1997; 79:1673–1676.
48. Schartl M, Bocksch W, Koschyk DH, et al. Use of intravascular ultrasound to compare effects of different strategies of lipid-lowering therapy on plaque volume and composition in patients with coronary artery disease. Circulation 2001; 104: 387–392.
49. Callister TQ, Cooil B, Raya SP, Lippolis NJ, Russo DJ, Raggi P. Coronary artery disease: improved reproducibility of calcium scoring with and electron-beam CT volumetric method. Radiology 1998; 208: 807–814.
50. Detrano R, Tang W, Kang X, et al. Accurate coronary calcium phosphate mass measurements from electron beam computed tomograms. Am J Card Imaging 1995; 9:167–173.
51. Rumberger JA, Simons DB, Fitzpatrick LA, Sheedy PF, Schwartz RS. Coronary artery calcium area by electron-beam computed tomography and coronary atherosclerotic plaque area. Circulation 1995; 92: 2157–2162.
52. Sangiorgi G, Rumberger JA, Severson A, et al. Arterial calcification and not lumen stenosis is highly correlated with atherosclerotic plaque burden in humans. J Am Coll Cardiol 1998; 31:126–133.
53. Secci A, Wong N, Tang W, Wang S, Doherty T, Detrano R. Electron beam computed tomographic coronary calcium as a predictor of coronary events. Circulation 1997; 96:1122–1129.
54. Callister TQ, Raggi P, Cooil B, Lippolis NJ, Russo DJ. Effect of HMG-CoA reductase inhibitors on coronary artery disease by electron-beam computed tomography. N Engl J Med 1998; 339:1972–1978.
55. Achenbach S, Ropers D, Pohle K, et al. Influence of lipid-lowering therapy on the progression of coronary artery calcification: a prospective evaluation. Circulation 2002; 106:1077–1082.
56. Bild DE, Bluemke DA, Burke GL, et al. Multi-ethnic study of atherosclerosis: objectives and design. Am J Epidemiol 2002; 156:871–881.
57. O'Rourke RA, Brundage BH, Froelicher VF, et al. American College of Cardiology/American Heart Association expert consensus document on electron-beam computed tomography for the diagnosis and prognosis of coronary artery disease. Circulation 2000; 102:126–140.
58. Schmermund A, Erbel R. Unstable coronary plaque and its relation to coronary calcium. Circulation 2001; 104:1682–1687.
59. Gussenhoven EJ, Essed CE, Lancee CT, et al. Arterial wall characteristics determined by intravascular ultrasound imaging: an in vitro study. J Am Coll Cardiol 1989; 14:947–952.
60. Hodgson JM, Reddy KG, Suneja R, Nair RN, Lesnefsky EJ, Sheehan HM. Intracoronary ultrasound imaging: correlation of plaque morphology with angiography, clinical syndrome and procedural results in patients undergoing coronary angioplasty. J Am Coll Cardiol 1993; 21:35–44.
61. Yamagishi M, Terashima M, Awano K, et al. Morphology of vulnerable coronary plaque: insights from follow-up of patients examined by intravascular ultrasound before and acute coronary syndrome. J Am Coll Cardiol 2000; 35:106–111.
62. Yabushita H, Bouma BE, Houser SL, et al. Characterization of human atherosclerosis by optical coherence tomography. Circulation 2002; 106:1640–1645.
63. Yuan C, Mitsumori LM, Ferguson MS, et al. In vivo accuracy of multispectral magnetic resonance imaging for identifying lipid-rich necrotic cores and intraplaque hemorrhage in advanced human carotid plaques. Circulation 2001; 104:2051–2056.